

Fig.3.6. Lorentzian profile centered at  $\omega' = \omega_0 - v_z/c$  which belongs to molecules with a definite velocity component  $v_z$

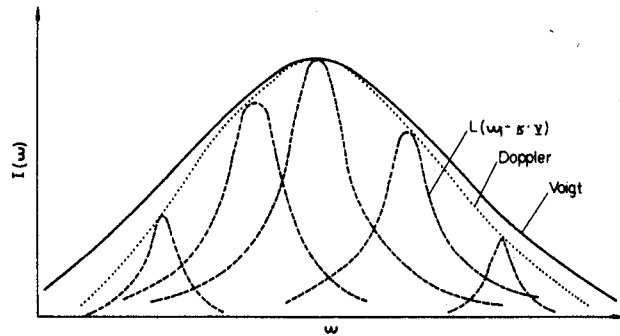


Fig.3.7. Voigt profile

with a central frequency  $\omega'$  (see Fig.3.6). Let  $n(\omega')d\omega' = n(v_z)dv_z$  be the number of molecules per unit volume with velocity components within the interval  $v_z$  to  $v_z + dv_z$ . The spectral intensity distribution  $I(\omega)$  of the total absorption or emission of all molecules at the transition  $E_i \rightarrow E_k$  is then

$$I(\omega) = I_0 \int n(\omega')g(\omega - \omega')d\omega' \quad (3.32)$$

Inserting (3.10) for  $g(\omega - \omega')$  and (3.28) for  $n(\omega')$  we obtain

$$I(\omega) = C \int_0^\infty \frac{e^{-[(c/v_p)(\omega_0 - \omega')/\omega_0]^2}}{(\omega - \omega')^2 + (\gamma/2)^2} d\omega' \quad \text{with} \quad C = \frac{\gamma N_i c}{2v_p n^{3/2} \omega_0} \quad (3.33)$$

This intensity profile, which is a convolution of Lorentzian and Gaussian profiles, [3.4] is called a *Voigt profile* (see Fig.3.7). Voigt profiles play

# Demtröder, Laser Spectroscopy

an important role in the spectroscopy of stellar atmospheres where accurate measurements of line wings allow the contributions of Doppler broadening and natural linewidth or collision line broadening to be separated (see next section and [3.5]). From such measurements the temperature and pressure of the emitting or absorbing layers in the stellar atmospheres may be deduced.

## 8.8.

### ~~8.8~~ Collision Broadening of Spectral Lines

When an atom A with energy levels  $E_i$  and  $E_k$  approaches another atom or molecule B, the energy levels of A are shifted because of the interaction between A and B. This shift depends on the electron configurations of A and B and on the distance  $R(A,B)$  between both collision partners, which, for definiteness, we define as the distance between the centers of mass of A and B.

The energy shifts  $\Delta E$  are in general different for the levels  $E_i$  and  $E_k$  and they may be positive as well as negative.  $\Delta E$  is positive if the interaction between A and B is repulsive and negative if it is attractive. When plotting the energy  $E(R)$  for the different energy levels as a function of the interatomic distance  $R$  the potential curves of Fig.3.8 are obtained.

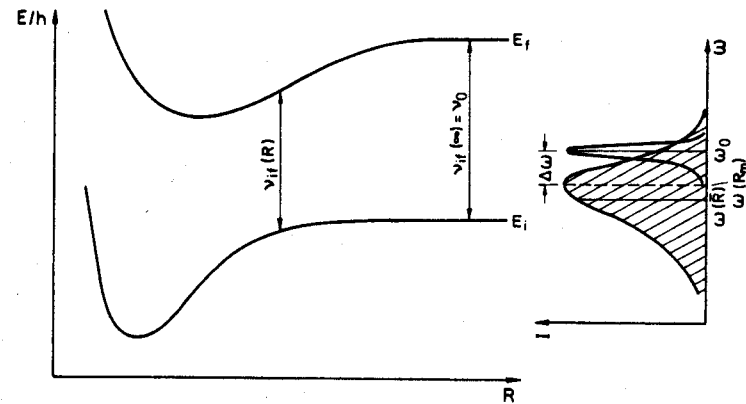


Fig.3.8. Illustration of collisional line broadening explained with the potential curves of the collision pair AB

This mutual interaction of both partners at distances  $R \leq R_c$  is called a *collision* and  $2R_c$  is the *collision diameter*. If no internal energy of the collision partners is transferred during the collision by nonradiative tran-

sitions, the collision is called *elastic*. Without additional stabilizing mechanisms (recombination) the partners will separate again after the collision time  $\tau_c \approx R_c/v$  which depends on the relative velocity  $v$ .

#### Numerical Example

$v = 5 \times 10^2$  m/s,  $R_c = 1$  nm  $\Rightarrow \tau_c = 2 \times 10^{-12}$  s. During this time the electronic charge distribution generally follows the perturbation "adiabatically", which justifies the potential curve model of Fig.3.8.

If atom A undergoes a *radiative* transition between levels  $E_i$  and  $E_k$  during the collision time, the frequency  $\omega_{ik}$  of absorbed or emitted radiation, satisfying

$$\hbar\omega_{ik} = |E_i(R) - E_k(R)|, \quad (3.34)$$

depends on the distance  $R(t)$  at the time  $t$  of the transition. We assume that the radiative transition takes place in a time interval short compared to the collision time, so that the distance  $R$  does not change during the transition. In Fig.3.8, this assumption leads to vertical radiative transitions.

In a gas mixture of atoms A and B the mutual distances  $R(A,B)$  show random fluctuations with a distribution around a mean value  $\bar{R}$  which depends on pressure and temperature. According to (3.34) the fluorescence shows a corresponding frequency distribution around a most probable value  $\overline{\omega_{ik}(R_m)}$  which may be shifted against the frequency  $\omega_0$  of the unperturbed atom A. The shift  $\Delta\omega = \omega_0 - \omega_{ik}$  depends on how differently the two energy levels  $E_i$  and  $E_k$  are shifted at a distance  $R_m(A,B)$  where the emission probability has a maximum. The intensity profile  $I(\omega)$  of the collision-broadened and shifted emission line can be obtained from

$$I(\omega) \propto \int A_{ik}(R) P_{col}(R) [E_i(R) - E_k(R)] dR, \quad (3.35)$$

where  $A_{ik}(R)$  is the spontaneous transition probability which depends on  $R$  because the electronic wave functions of the collision pair (AB) depend on  $R$ , and  $P_{col}(R)$  is the probability per unit time that the distance between A and B lies in the range from  $R$  to  $R + dR$ .

From (3.35) it can be seen that the intensity profile of the collision-broadened line reflects the difference of the potential curve

$$E_i(R) - E_k(R) = V[A(E_i), B] - V[A(E_k), B].$$

The line shift is caused by elastic collisions as will be shown below. The energy defect  $\Delta E = \hbar\Delta\omega$  is supplied from the kinetic energy of the collision

partners. This means that in case of positive shifts ( $\Delta\omega > 0$ ), the kinetic energy is smaller after the collision than before.

Besides elastic collisions, inelastic collisions may also occur in which the excitation energy  $E_i$  of atom A is either partly or completely transferred into internal energy of the collision partner B or into translational energy of both partners. Such inelastic collisions are often called *quenching collisions* because they decrease the number of excited atoms in level  $E_i$  and therefore quench the fluorescence intensity. According to Sect.2.7.1, the total transition probability  $A_i$  for the depopulation of level  $E_i$  is a sum of spontaneous and collision-induced probabilities. Using the relation

$$p_B = N_B kT \quad (3.36)$$

between density  $N_B$  and pressure  $p_B$  of the collision partner B, one obtains from (2.82) with  $\rho_{ik} = 0$  the total transition probability

$$A_i^{eff} = \sum_k A_{ik} + a p_B \quad \text{with} \quad a = \sigma_{ik}^{col} \frac{(2kT)^{3/2}}{(\pi\mu)^{1/2}}. \quad (3.37)$$

It is evident from (3.24) that this pressure-dependent transition probability causes a corresponding pressure-dependent linewidth  $\delta\omega$  which is proportional to the pressure  $p$  of the collision partners and which can be described by a sum of two damping terms

$$\delta\omega = \delta\omega_n + \delta\omega_{col} = \gamma_n + \gamma_{col} = \gamma_n + a p. \quad (3.38)$$

The collision-induced additional line broadening is therefore often called *pressure broadening*.

The preceding discussion has shown that both elastic and inelastic collisions cause spectral line broadening. The elastic collisions may additionally cause a line shift which depends on the potential curves  $E_i(R)$  and  $E_k(R)$ . This can be quantitatively seen from a model introduced by LINDHOLM [3.6], which treats the excited atom A as a damped oscillator which suffers collisions with particles B (atoms or molecules). In this model inelastic collisions damp the *amplitude* of the oscillation. This is described by introducing a damping constant  $\gamma_{col}$  such that the sum of radiative and collisional damping is represented by  $\gamma = \gamma_n + \gamma_{col}$ . From the derivation in Sect.3.1 one obtains for the line broadened by inelastic collisions a Lorentzian profile with halfwidth (3.38)

$$I(\omega) = \frac{C}{(\omega - \omega_0)^2 + [(\gamma_n + \gamma_{col})/2]^2}.$$

The elastic collisions change not the *amplitude*, but the *phase* of the damped oscillator, due to the frequency shift  $\Delta\omega(R)$  during the collisions. They are often called *phase-perturbing collisions*. We now give a short outline of a quantitative description based on this model which gives a better insight into the relation between line profile and collision cross sections [3.7,8].

As in Sect.3.1, we describe the damped oscillatory by its time-dependent amplitude

$$x(t) = x_0 e^{i\omega_0 t + i\eta(t) - \gamma t/2}, \quad (3.39)$$

in which  $\gamma = \gamma_n + \gamma_{col}$  includes both radiative damping and damping by inelastic collisions. The term

$$\eta(t) = \int_0^t [\omega(t) - \omega_0] dt = \int_0^t \Delta\omega(t) dt \quad (3.40)$$

represents the sum of all phase shifts of our oscillator due to all collisions within the time from 0 to  $t$ . We shall at first neglected the damping by radiative transitions and inelastic collisions and treat the elastic collisions separately, so that  $\gamma = 0$  in (3.39).

When the integration time is long compared to the mean time  $T = \Lambda/\bar{v}$  between successive collisions (which depends on the mean free path  $\Lambda$  and the mean relative velocity  $\bar{v}$ ) the total phase shift  $\eta(t)$  is the sum of many random phase shifts caused by collisions with different impact parameters (see Fig.3.9). The mean phase shift per collision depends on the correlation between the oscillation before and after the collisions, which can be described by the correlation function

$$\begin{aligned} \varphi(\tau) &= \frac{1}{x_0^2} e^{-i\omega_0 \tau} \lim_{t \rightarrow \infty} \frac{1}{t} \int_{-t/2}^{+t/2} x^*(t) x(t + \tau) dt \\ &= \lim_{t \rightarrow \infty} \frac{1}{t} \int_{-t/2}^{+t/2} e^{i[\eta(t+\tau) - \eta(t)]} dt \end{aligned} \quad (3.41)$$

During the time interval  $d\tau$  the change of  $\varphi(\tau)$  depends on the number of collisions and on the mean phase jump per collision. What is the physical meaning of  $\varphi(\tau)$ ?

From (3.41) we obtain

$$x_0^2 \int_{-\tau/2}^{+\tau/2} \varphi(\tau) e^{i(\omega_0 - \omega)\tau} d\tau = \lim_{t \rightarrow \infty} \frac{1}{t} \int_{-t/2}^{+t/2} x^*(t) e^{i\omega t} \int_{-\tau/2}^{+\tau/2} x(t + \tau) e^{-i\omega(t+\tau)} d\tau \quad (3.42)$$

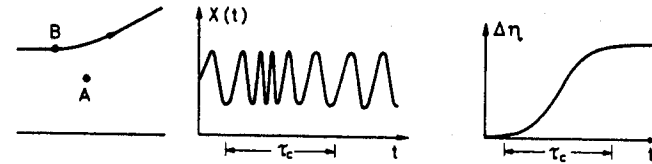


Fig.3.9. Phase perturbations of an oscillator by collisions

The integral over  $d\tau$  does not depend on our choice of time origin. We may therefore shift the time scale by an amount  $\tau$  from  $t + \tau$  to  $t$  (see the analogous discussion in Sect.2.9.4). Replacing the dummy variable  $\tau$  on the right-hand side of (3.42) by  $t$  we can write

$$\begin{aligned} x_0^2 \lim_{t \rightarrow \infty} \frac{1}{2\pi} \int_{-\tau/2}^{+\tau/2} \varphi(\tau) e^{i(\omega_0 - \omega)\tau} d\tau &= \lim_{t \rightarrow \infty} \frac{1}{2\pi t} \int_{-t/2}^{+t/2} x^*(t) e^{i\omega t} dt \int_{-t/2}^{+t/2} x(t) e^{-i\omega t} dt \\ &= \text{F.T.}(xx^*) = I(\omega) \end{aligned} \quad (3.43)$$

The right-hand side of (3.43) is just the *Fourier transform of the square of the amplitude*  $X^*(t)X(t)$  and represents therefore the *intensity profile*  $I(\omega)$  of the *spectral line* (see also Sect.3.1). Provided that we know the correlation function  $\varphi(\tau)$  we can use (3.43) to determine the line profile produced by the elastic collisions. This can be performed as follows.

With

$$\Delta\eta = \eta(t + \tau) - \eta(t), \quad (3.44)$$

we can write

$$\varphi(\tau) = \lim_{t \rightarrow \infty} \frac{1}{t} \int_{-t/2}^{+t/2} e^{i\Delta\eta} dt = \langle e^{i\Delta\eta(\tau)} \rangle \quad (3.45)$$

the increment  $d\varphi(\tau)$  during the time interval  $d\tau$  is

$$\begin{aligned} d\varphi(\tau) &= \varphi(\tau + d\tau) - \varphi(\tau) = \langle e^{i\Delta\eta(\tau+d\tau)} \rangle - \langle e^{i\Delta\eta(\tau)} \rangle \\ &= \langle e^{i\Delta\eta(\tau)} (e^{i\epsilon} - 1) \rangle, \end{aligned} \quad (3.46)$$

where  $\epsilon$  stands for the additional phase shift during the time interval  $d\tau$ . When the phase jump occurring at a collision is independent of the phase  $\eta$  before the collision, we can replace the time average of the product by the product of the averaged factors, which gives

$$d\varphi(\tau) = \langle e^{i\Delta\eta(\tau)} \rangle \langle e^{i\epsilon} - 1 \rangle = \varphi(\tau) \langle e^{i\epsilon} - 1 \rangle. \quad (3.47)$$

We can further replace the time average by an ensemble average which is equivalent to an average over all possible collisions [3.9].

In a gas with  $N$  particles per unit volume, during the time interval  $d\tau$  our oscillator suffers

$$dZ = 2\pi R dR N \bar{v} d\tau \quad (3.48)$$

collisions with impact parameters between  $R$  and  $R + dR$ , where  $\bar{v}$  is the mean relative velocity. The ensemble average  $\langle \exp(i\epsilon) - 1 \rangle$  is therefore

$$\begin{aligned} \langle e^{i\epsilon} - 1 \rangle &= 2\pi N \bar{v} d\tau \int_0^\infty \langle e^{i\eta(R)} - 1 \rangle R dR \\ &= N \bar{v} d\tau (\sigma_b - i\sigma_s) \end{aligned} \quad (3.49)$$

with the abbreviations

$$\sigma_b = 2\pi \int_0^\infty [1 - \cos\eta(R)] R dR \quad (3.50)$$

$$\sigma_s = 2\pi \int_0^\infty [\sin\eta(R)] R dR \quad (3.51)$$

Integration of (3.46) yields the correlation function

$$\phi(\tau) = e^{-N\bar{v}\tau(\sigma_b - i\sigma_s)} \quad (3.52)$$

By substituting (3.52) into (3.43) we finally obtain the line profile

$$I(\omega) = I_0 \frac{N\bar{v}\sigma_b}{(\omega - \omega_0 - N\bar{v}\sigma_s)^2 + (N\bar{v}\sigma_b)^2} \quad (3.53)$$

which shows that the line profile in the presence of elastic collisions is a Lorentzian with a halfwidth

$$\delta\omega = 2N\bar{v}\sigma_b \quad (3.54)$$

and a shift of the line center

$$\Delta\omega = N\bar{v}\sigma_s \quad (3.55)$$

In this model of the phase-perturbed oscillator, both line broadening and line shift are proportional to the density  $N$  of collision partners and to the mean relative velocity  $\bar{v}$ . The line broadening is determined by the cross section  $\sigma_b$  (3.50) and the line shift by  $\sigma_s$  (3.51).

If we now include additional damping by spontaneous emission of the oscillator and by inelastic collisions, we can consider these effects on the line profiles by introducing into (3.53) the damping constant  $\gamma = \gamma_n + \gamma_{col}^{ine}$  and obtain the Lorentzian profile of a damped oscillator which suffers elastic and inelastic collisions.

$$I(\omega) = I_0 \frac{(\gamma_n/2 + \gamma_{col}^{ine}/2 + N\bar{v}\sigma_b)^2}{(\omega - \omega_0 - N\bar{v}\sigma_s)^2 + [(\gamma_n + \gamma_{col}^{ine})/2 + N\bar{v}\sigma_b]^2} \quad (3.56)$$

In order to gain more insight into the physical meaning of the cross sections  $\sigma_s$  and  $\sigma_b$  we have to discover the relation between the phase shift  $\eta(R)$  and the potential  $V(R)$ . Assume a potential of the form

$$V_i(R) = C_i/R^n \quad (3.57)$$

between the atom in level  $E_i$  and the perturbing atom B. The frequency shift  $\Delta\omega$  for the transition  $E_i \rightarrow E_k$  is then

$$\mathcal{H}\Delta\omega(r) = \frac{C_i - C_k}{R^n} \quad (3.58)$$

and the corresponding phase shift for a collision with impact parameter  $R_0$ , where we neglect the scattering of B and assume that the path of B is not deflected but follows a straight line (Fig.3.10), is

$$\eta(R_0) = \int_{-\infty}^{+\infty} \Delta\omega dt = \int \frac{(C_i - C_k) dt}{[R_0^2 + \bar{v}^2(t - t_0)^2]^{n/2}} = \frac{\alpha_n(C_i - C_k)}{\bar{v}R_0^{n-1}} \quad (3.59)$$

Equation (3.59) shows the relation between phase shift  $\eta(R_0)$  and the interaction potential (3.57), where  $\alpha_n$  is a numerical constant depending on the exponent  $n$  in (3.57).

Substituting  $\eta(R)$  into (3.50) and (3.51) allows the cross sections  $\sigma_s$  and  $\sigma_b$  to be calculated. The calculation for  $n = 4$ , for example, yields the result that the main contribution to  $\sigma_b$  comes from collisions with *small* impact parameters whereas  $\sigma_s$  still has large values for *large* impact parameters. This means that *collisions at large distances do not cause noticeable broadening of the line but can still very effectively shift the line center.*

From the preceding discussion it might appear that only the *difference*  $V_i(R) - V_k(R)$  of the interaction potentials between B and the atom A in its

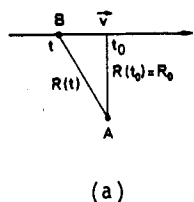
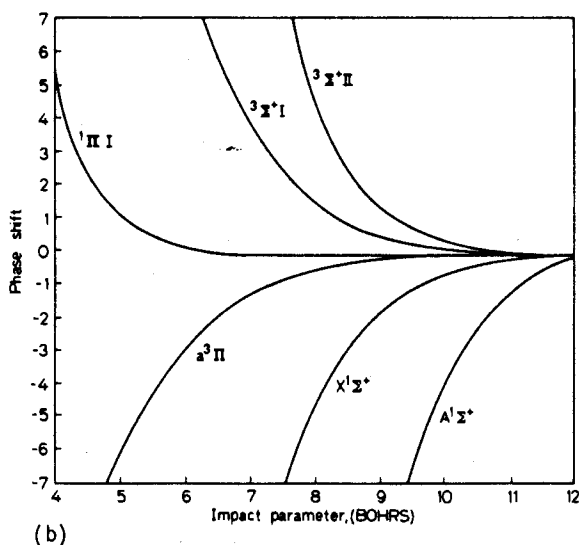


Fig.3.10. (a) Linear path approximation of a collision between A and B. (b) Phase shift versus impact parameter for Na-H collisions. The various adiabatic molecular states associated with  $\text{Na}^*(3P)$  are indicated [3.10]



two states  $E_i$  and  $E_k$  can be obtained from line broadening and line shifts. However, it is also possible to obtain separately the upper and lower potentials as follows:

Assume an interaction potential  $V(R)$  between atom A in its ground state and its collision partner B. The probability that B has a distance between  $R$  and  $R + dR$  is proportional to  $4\pi R^2 dR$  and (in thermal equilibrium) to the Boltzmann factor  $\exp[-V(R)/kT]$ . The density  $n(R)$  of collision pairs A, B with distance  $R$  is therefore

$$n_{AB}(R)dR = CR^2 e^{-V(R)/(kT)} dR \quad (3.60)$$

Because the intensity of an absorption line is proportional to the density of absorbing atoms while they are forming collision pairs, using the relation  $\mathcal{H}(\omega) = [V_i(R) - V_k(R)] \Rightarrow \mathcal{H}d\omega/dR = d[V_i(R) - V_k(R)]/dR$ , the intensity profile of the absorption line can be written as

$$I(\omega)d\omega = C^* \left\{ R^2 \exp\left(-\frac{V_i(R)}{kT}\right) \frac{d}{dR} [V_i(R) - V_k(R)] \right\} dR \quad (3.61)$$

Measuring the line profile as a function of temperature yields  $V_i(R)$  separately. Frequently, different spherical model potentials  $V(R)$  are substituted in (3.61) such as the potential (3.57) or the Lennard-Jones potential

$$V(R) = a/R^{12} - b/R^6 \quad (3.62)$$

and the coefficients  $c_i$  [for (3.57)] or  $a, b$  [for (3.62)] are adjusted for optimum agreement between theory and experiment [3.11,12].

Because of the long-range Coulomb interactions between charged particles (electrons and ions) described by the potential (3.57) with  $n = 1$ , pressure broadening and shift is particularly large in plasmas and gas discharges. The interaction between charged particles can be described by the linear and quadratic Stark effects. It can be shown that the linear Stark effect causes only line broadening, while the quadratic effect leads also to line shifts. From measurements of line profiles in plasmas, very detailed plasma characteristics, such as electron or ion densities and temperatures, can be determined. Plasma spectroscopy has therefore become an extensive field of research, of interest not only for astrophysics, but also for fusion research in high-temperature plasmas [3.13].

The classical models used to explain collision broadening and line shifts can be improved by using quantum mechanical calculations. These are, however, beyond the scope of this book, and the reader is referred to the literature [3.8-16].

#### Examples

- 1) The pressure broadening of the sodium D line  $\lambda = 589 \text{ nm}$  by argon is  $3 \times 10^{-4} \text{ \AA/torr}$ , equivalent to 30 MHz/torr. The shift is about minus 1 MHz/torr. The self-broadening of 150 MHz/torr, due to collision between Na atoms, is much larger. However, at pressures of several torr, the pressure broadening is still smaller than the Doppler width.
- 2) The pressure broadening of molecular vibration-rotation transitions with wavelengths  $\lambda \approx 5 \text{ }\mu\text{m}$  is a few MHz/torr. At atmospheric pressure, the collision broadening therefore exceeds the Doppler width. For example, the rotational lines of the  $\nu_2$  band of  $\text{H}_2\text{O}$  in air at normal pressure (760 torr) have a Doppler width of 150 MHz but a pressure-broadened line-width of 930 MHz.
- 3) The collision broadening of the red neon line at  $\lambda = 633 \text{ nm}$  in the low-pressure discharge of a He-Ne laser is about  $\delta\nu = 150 \text{ MHz/torr}$ ; the pressure shift  $\Delta\nu = 20 \text{ MHz/torr}$ . In high-current discharges, such as the argon laser discharge, the degree of ionization is much higher than in the He-Ne laser and the Coulomb interaction between ions and electrons plays a major role. The pressure broadening is therefore much larger:  $\delta\nu = 1500 \text{ MHz/torr}$ . Because of the high temperature in the plasma, the Doppler width  $\delta\nu_D \approx 5000 \text{ MHz}$  is yet still larger [3.17].

	Helium		Neon		Argon		Krypton		Xenon		Nitrogen		Carbon tetrafluoride	
	Width	Shift	Width	Shift	Width	Shift	Width	Shift	Width	Shift	Width	Shift	Width	Shift
Na 5896 P <sub>1/2</sub>					0.742	-0.196					0.49	-0.214		
Na 5890 P <sub>3/2</sub>					0.689	-0.213					0.49	-0.223		
K 7699 P <sub>1/2</sub>					1.01	-0.42					0.82	-0.36		
K 7665 P <sub>3/2</sub>					1.01	-0.36					0.82	-0.30		
K 4047 P <sub>1/2</sub>	1.45		0.71		2.20	-9.2					1.65	-0.83		
K 4044 P <sub>3/2</sub>	2.02		0.82	-0.16	2.58	-8.3					1.89	-1.02		
Rb 7947 P <sub>1/2</sub>	0.595	+0.228			0.627									
Rb 7800 P <sub>3/2</sub>	0.735	-0.092			0.855									
Rb 4216 P <sub>1/2</sub>	2.77	+0.93	1.30	+0.22	2.21	-1.2					1.51			
Rb 4202 P <sub>3/2</sub>	1.88	+0.43	0.73	-0.16	2.56	-1.0					1.01			
Cs 8943 P <sub>1/2</sub>		+0.128		-0.04	0.30	-0.238	0.28	-0.20	0.49	-0.25				-0.29
Cs 8521 P <sub>3/2</sub>		+0.015		-0.08	0.30	-0.215	0.28	-0.20	0.23	-0.25				-0.23
Cs 4593 P <sub>1/2</sub>		-0.51				-0.70	1.1	-0.62		-0.65				
Cs 4555 P <sub>3/2</sub>		-0.26				-0.63	3.2	-0.62		-0.65				

(a)

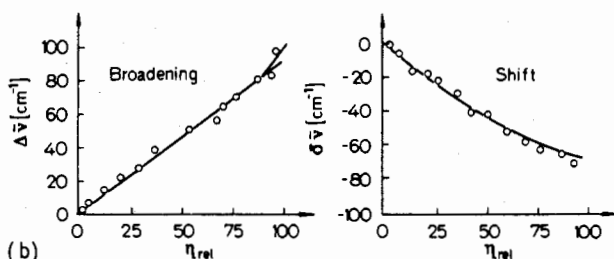


Fig.3.11. (a) Pressure broadening and shifts of some alkali resonance lines by different gases. The numbers are given in  $\text{cm}^{-1}$  for standard conditions (1 atm,  $15^\circ\text{C}$ ). (b) Halfwidth and line shift (in  $\text{cm}^{-1}$ ) of the Cs line  $\lambda = 894.3 \text{ nm}$  as a function of relative argon densities (density  $n$  at pressure  $p$  divided by the density at standard conditions) [3.2]

4) Figure 3.11a gives as examples pressure broadening and shifts of some alkali resonance lines perturbed by different gases. The numbers are in  $\text{cm}^{-1}$  at standard conditions of 1 atm and  $15^\circ\text{C}$ .

Figure 3.11b gives the halfwidth and line shift of the Cs line  $\lambda = 894.3 \text{ nm}$  in  $\text{cm}^{-1}$  as a function of relative density (i.e., density divided by density at 1 atm [3.2]).

#### Note

In the infrared and microwave range, collisions may sometimes cause a narrowing of the linewidth instead of a broadening (Dicke narrowing). This can be explained as follows. If the life time of the upper molecular level (e.g., an excited vibrational level in the electronic ground state) is long compared to the mean time between successive collisions, the velocity of the

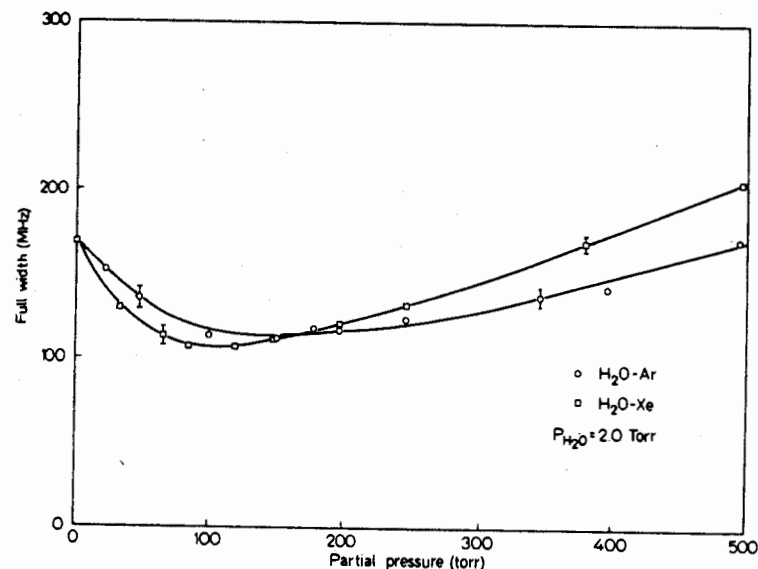


Fig.3.12. Dicke narrowing and pressure broadening of a rotational transition in  $\text{H}_2\text{O}$  at  $1871 \text{ cm}^{-1}$ , as a function of Ar and Xe pressure [3.18]

oscillator is often altered by elastic collisions and the mean velocity component is smaller than without these collisions, resulting in a smaller Doppler shift. When the Doppler width is larger than the pressure-broadened width, this causes a narrowing of the lines, if the mean free path is smaller than the wavelength of the molecular transition [3.18]. Figure 3.12 illustrates this "Dicke narrowing" for a rotational transition of the  $\text{H}_2\text{O}$  molecule at  $1871 \text{ cm}^{-1}$ . The linewidth decreases with increasing pressure up to pressures of about 100-150 torr, depending on the collision partner, which determines the mean free path  $\lambda$ . For higher pressures, the pressure broadening overcompensates the Dicke narrowing, and the linewidth increases again.

#### 3.4 Time-of-Flight Broadening

In many experiments in laser spectroscopy, the interaction time of molecules with the radiation field is small compared with the spontaneous lifetimes of excited levels. Particularly for transitions between rotational-vibrational levels of molecules with spontaneous lifetimes in the millisecond range, the time of flight  $T = d/\bar{v}$  of molecules with a mean thermal velocity  $\bar{v}$  through a laser beam of diameter  $d$  may be smaller than the spon-